DEUTSCHES ELEKTRONEN-SYNCHROTRON
Ein Forschungszentrum der Helmholtz-Gemeinschaft

DESY 21-165
arXiv:2111.02453
November 2021

Bootstrapping (D, D) Conformal Matter

F. Baume

Department of Physics and Astronomy,
University of Pennsylvania, Philadelphia, USA

C. Lawrie

Deutsches Elektronen-Synchrotron DESY, Hamburg

and

Department of Physics and Astronomy,
University of Pennsylvania, Philadelphia, USA

ISSN 0418-9833

NOTKESTRASSE 85 - 22607 HAMBURG

Herausgeber und Vertrieb:

Verlag Deutsches Elektronen-Synchrotron DESY

DESY Bibliothek
Notkestr. 85
22607 Hamburg
Germany

Bootstrapping (D, D) Conformal Matter

Florent Baume*
Department of Physics and Astronomy, University of Pennsylvania, Philadelphia, PA 19104, USA

Craig Lawrie†
Deutsches Elektronen-Synchrotron DESY, Notkestr. 85, 22607 Hamburg, Germany and
Department of Physics and Astronomy, University of Pennsylvania, Philadelphia, PA 19104, USA

We use the numerical conformal bootstrap to study six-dimensional $\mathcal{N} = (1, 0)$ superconformal field theories with flavor symmetry $\mathfrak{so}_{4k}$. We present evidence that minimal (D_k, D_k) conformal matter saturates the unitarity bounds for arbitrary k. Furthermore, using the extremal-functional method, we check that the chiral-ring relations are correctly reproduced, extract the anomalous dimensions of low-lying long superconformal multiplets, and find hints for novel OPE selection rules involving type-$\mathcal{B}$ multiplets.

I. INTRODUCTION

For the last three decades, string theory has been a potent apparatus for the construction of quantum field theories (QFTs). The power of this approach finds its source in the way the parameters and properties of the quantum field theory are governed by geometrical and topological features of the compactification space. Conformal field theories (CFTs) are an especially interesting class of QFTs; they exist at the fixed points of the renormalization group flows, and thus they can provide important insights into the nature of quantum field theory.

In this work, our focus is on CFTs with additional supersymmetry, known as superconformal field theories (SCFTs). From a pure field theory perspective, it was long unknown whether interacting superconformal field theories exist in five or six dimensions, despite the existence of the appropriate superconformal algebras [1]. In part, the challenge in constructing such theories lies in the fact that there are no supersymmetry-preserving marginal deformations in five or six dimensions [2], and thus the usual techniques of perturbation theory cannot be applied. In the 1990s, it was discovered that compactifications of Type IIB string theory on non-compact K3 surfaces give rise to exotic six-dimensional theories, with sixteen supercharges, whose constituent objects are tensionless strings [3], and it was soon realized that they are in fact superconformal field theories [4]. This is a prime example of *geometric engineering*; each such 6d SCFT is associated to a finite subgroup of $SU(2)$, Γ, as the K3 surfaces are all locally of the orbifold form $\mathbb{C}^2/\Gamma$.

One of the recent successes of this technique of geometric engineering of quantum field theories is the enumeration of a vast landscape of six-dimensional superconformal field theories with eight supercharges obtained via F-theory [5, 6]. The SCFTs realized by this construction have a quiver-like structure; the "links" appearing in these quivers are themselves non-trivial interacting SCFTs with a $\mathfrak{g} \oplus \mathfrak{g}'$ flavor algebra – they are a generalization of an $\mathfrak{su}_n \oplus \mathfrak{su}_m$ bifundamental hypermultiplet – known as minimal $(\mathfrak{g}, \mathfrak{g}')$ conformal matter [7]. These conformal matter theories have a simple construction from the perspective of M-theory: for each ADE algebra $\mathfrak{g}' = \mathfrak{g}$, the minimal conformal matter theory lives on the worldvolume of a single M5-brane probing a $\mathbb{C}^2/\Gamma$ orbifold, where Γ is the finite subgroup of $SU(2)$ of the same ADE-type as $\mathfrak{g}$.

Despite marking a significant milestone in our understanding of six-dimensional field theories, it remains unknown to what extent the landscape of consistent 6d SCFTs matches that obtained from geometric constructions. There are six-dimensional SCFTs which are constructed with "frozen" 7-branes, and these are not captured by the geometric constructions of [5, 6], however such SCFTs may still be obtainable from an F-theory origin [8, 9]. Similarly, there are putative 6d SCFTs that appear non-anomalous from the bottom-up, field-theoretic perspective, however there is no known way to engineer these theories from F-theory; such theories are widely believed to be inconsistent for a variety of indirect reasons [10, 11], however this has not been rigorously established. As a final example, there is a seemingly consistent spectrum with $\mathfrak{su}_3$ flavor symmetry, for which the Higgs branch is the one-instanton moduli space of $SU(3)$ [12]; this theory does not have a known geometric construction. It is an open question, which can be considered as part of the swampland program, whether all consistent 6d SCFTs have an origin in string theory.

The main drawback of the geometric engineering approach is that, up to a small collection of protected quantities such as the central charges, it is unknown how to access the conformal data, namely the conformal dimensions and OPE coefficients, from the geometry. This raises the question of whether other techniques, when used in conjunction with geometry, can be employed

* email: fbaume@sas.upenn.edu
† gmail: craig.lawrie1729

to learn about those conformal quantities. Some work towards the determination of the conformal dimensions for certain classes of unprotected operators in 6d $(1,0)$ SCFTs was initiated in [13, 14].

Concurrently, but transversely, to the development of the geometric program, the conformal bootstrap [15, 16] has known renewed interest, sparked in [17], and provides a technique for bounding the conformal data of a CFT. Using the associativity of the operator product expansion (OPE), the ethos of the bootstrap is to harness the power of unitarity to impose strict bounds on the values that the conformal data of a(n S)CFT can take, with minimal assumptions on the spectrum of the theory. The superconformal bootstrap has been applied to SCFTs with at least eight supercharges; in three [18–23] and four [24–37] dimensions there is a significant body of literature, however five [38] and six [39–41] dimensional analyses have been carried out comparatively less. In general, the bounds that are imposed by crossing symmetry and associativity of the OPE appear to be saturated by SCFTs that have a construction via string theory. While most of the literature has focused on theories in lower dimensions, the geometric landscape of 6d $(1,0)$ SCFTs that has been charted in [5, 6] is opportune for exploitation via bootstrap techniques.

In this paper, we use the numerical conformal bootstrap to study six-dimensional $\mathcal{N}=(1,0)$ SCFTs with a non-Abelian flavor symmetry. We focus on those with flavor algebra $\mathfrak{so}_{4k}$, for $k>4$. We find that the lower bound imposed by unitarity on the flavor central charge for a given value of k converges to that of minimal (D_k, D_k) conformal matter. This suggests that such conformal matter is the "smallest" SCFT with that flavor symmetry, and rules out any potential more exotic theory with a smaller flavor central charge. Assuming that the bound is saturated, we proceed to extract the conformal dimensions of the first few scalar long multiplets. We observe that the half-BPS multiplets that appear to be absent from the spectrum are consistent with those known to be projected out by the Higgs-branch chiral ring of minimal (D_k, D_k) conformal matter, providing further confirmation for the conjecture that conformal matter saturates the bounds.

II. MINIMAL (D_k, D_k) CONFORMAL MATTER

Before discussing how the conformal bootstrap can be used to learn about the data of 6d SCFTs, we review how they can be engineered in F-theory, and in particular how minimal (D_k, D_k) conformal matter and some of its properties arise from geometry.

Six-dimensional theories with superconformal symmetry are obtained by compactification of F-theory on particular non-compact elliptically-fibered Calabi–Yau threefolds. The internal space encodes many properties of the theory, including the required cancellation of gauge anomalies.[1] As mentioned in the introduction, an extra ingredient in six-dimensional conformal theories is the presence of tensionless strings in their spectrum – and the tensor multiplets they magnetically couple to – which are absent in their lower-dimensional cousins. These can be realized by wrapping D3-branes on curves in the base of the elliptic fibration, where the tension of the string is set by the volume of the curve. To obtain an SCFT it is therefore necessary that there are no curves of finite volume, as they would otherwise introduce a scale induced by the tension.

In practice, one can begin by enumerating all non-compact bases containing configurations of contractible curves such that there exists a minimal elliptic fibration over them. Compactification of F-theory on these geometries however gives rise to 6d field theories containing tensionful strings. This geometry corresponds to the tensor branch of a 6d SCFT if it is possible to simultaneously shrink all rigid curves to zero volume; this can be done if the intersection matrix of the curves – corresponding to the Dirac pairing of the 6d strings – is negative definite. This condition, in addition to the requirement that the elliptic fibration has only minimal singularities, makes it possible to enumerate all such tensor-branch geometries leading to an SCFT [5, 6].

In this top-down approach, minimal (D_k, D_k) conformal matter is realized through an elliptic fibration over $\mathbb{C}^2$. The elliptic fiber over a generic point is a smooth torus, and over two divisors, z_1 and z_2, in $\mathbb{C}^2$ there exist I^{*s}_{k-4} singular fibers.[2] These singular fibers make manifest an $\mathfrak{so}_{2k} \oplus \mathfrak{so}_{2k}$ flavor algebra. The tensor-branch geometry is obtained by blowing up the intersection point in $\mathbb{C}^2$ between the divisors z_1 and z_2. This procedure introduces a compact (-1)-curve over which the singular fiber is I^{ns}_{k-4}, corresponding to an $\mathfrak{sp}_{k-4}$ gauge algebra.[3] This tensor-branch geometry can be compactly written in the shorthand notation

$$\overset{\mathfrak{sp}_{k-4}}{1} \quad . \tag{1}$$

On the tensor branch the theory has the following content: one tensor multiplet; a vector multiplet in the adjoint representation of $\mathfrak{sp}_{k-4}$; and $4k$ half-hypermultiplets in the fundamental representation of $\mathfrak{sp}_{k-4}$. As the fundamental representation of the gauge algebra is pseudo-real, the $4k$ half-hypermultiplets are rotated by a classical $\mathfrak{so}_{4k}$ flavor symmetry, and this indicates that the

[1] For a recent review of the construction and properties of 6d SCFTs that arise from F-theory, see [42].

[2] For the notation for the types of singular fibers in elliptically-fibered Calabi–Yau threefolds, we refer the reader to [43].

[3] The case $k=4$ corresponds to having no gauge algebra over the (-1)-curve; this is the geometric configuration associated to the E-string theory, and the flavor symmetry enhances: $\mathfrak{so}_8 \oplus \mathfrak{so}_8 \to \mathfrak{e}_8$. We will assume $k>4$ in this article. The superconformal bootstrap for the E-string has been studied in [40].

geometrically-manifest flavor algebra is enhanced:

$$\mathfrak{so}_{2k} \oplus \mathfrak{so}_{2k} \to \mathfrak{so}_{4k} \,. \tag{2}$$

This $\mathfrak{so}_{4k}$ is the flavor symmetry of the gauge theory that exists on the generic point of the tensor branch. We can verify that $\mathfrak{so}_{4k}$ is also the flavor symmetry of the SCFT at the origin of the tensor branch by studying, for example, the infinite-coupling magnetic quiver [44].

Our knowledge of the conformal data, such as the scaling dimensions and OPE coefficients, of the 6d SCFTs constructed from geometry in the manner that we have just described remains limited. While the SCFT may possess a weakly-coupled regime away from the fixed point, one of the obstacles is that it is generally unknown how to fully track data obtained using such a description, e.g. the gauge-invariant operators on the tensor branch, to the origin where the SCFT resides. From the geometry, we are however able to compute a particular set of symmetry-protected quantities on the tensor branch, and follow them through the geometric deformations that lead to the origin in a controlled way.

One such quantity is the anomaly polynomial. Moving onto the tensor branch, where the scalar fields inside the tensor multiplets receive non-trivial vacuum expectation values, conformal invariance is broken. However, since these scalars are uncharged under the other symmetries, conformality is the only symmetry which is broken. As such, one can use a form of 't Hooft anomaly matching to determine the anomaly polynomial of the SCFT at the conformal fixed point [45, 46].

For a theory in d dimensions, the anomaly polynomial is a formal $(d+2)$-form which captures the variation of the partition function under the application of a symmetry transformation via the Wess–Zumino descent procedure. In 6d, it is generally written in terms of the characteristic classes of the bundles associated to the gravitational, flavor, and $SU(2)_R$ symmetries; it measures an obstruction to the gauging of these symmetries.[4] The $(1,0)$ supersymmetry mandates that various coefficients appearing in the anomaly polynomial can be related to the central charges of the theory, and these can further be related to certain OPE coefficients. The bounds derived on the OPE coefficients from the conformal bootstrap then lead to bounds on quantities which can be obtained geometrically from the anomaly polynomial.

The anomaly polynomial for a 6d SCFT contains the terms

$$I_8 = \sum_a \mathrm{Tr} F_a^2 \big(\kappa_a p_1(T) + \nu_a c_2(R)\big) + \cdots \,, \tag{3}$$

where $p_1(T)$ is the first Pontryagin class of the tangent bundle to the six-dimensional spacetime, $c_2(R)$ is the second Chern class of the $SU(2)_R$ R-symmetry bundle, and $\mathrm{Tr} F_a^2$ is the curvature of each flavor symmetry bundle. The index a runs over all simple non-Abelian flavor symmetries.

It has been shown in [40, 48] that the flavor central charges, which are defined through the two-point correlation function of the flavor currents,[5]

$$\big\langle J_\mu^a(x) J_\nu^b(0)\big\rangle = \frac{(C_J)_a}{\mathrm{vol}(S^5)^2}\,\delta^{ab}\,\frac{x^2\eta_{\mu\nu} - 2x_\mu x_\nu}{x^{12}} \,, \tag{4}$$

can be written in terms of the 't Hooft coefficients of the anomaly polynomial via

$$(C_J)_a = 240\,(\kappa_a - \nu_a) \,. \tag{5}$$

In the F-theory construction, the anomaly polynomial can be determined from the geometric data of the associated non-compact elliptically-fibered Calabi–Yau, together with (mixed-)gauge anomaly cancellation. For (D_k, D_k) conformal matter it was worked out in [45], using the tensor-branch geometry as in equation (1), and the relevant coefficients from the anomaly polynomial were found to be

$$\nu = -\frac{1}{4}(k-3) \,, \qquad \kappa = \frac{1}{48}(k-1) \,. \tag{6}$$

As the theory has only a single simple flavor symmetry factor, $\mathfrak{so}_{4k}$, we have suppressed the index a. From the relation (5) we can immediately see that the flavor central charge is[6]

$$C_J = 65(k-4) + 75 \,. \tag{7}$$

The flavor current associated to a flavor symmetry of a 6d $\mathcal{N} = (1,0)$ SCFT belong to the half-BPS superconformal multiplet known as a $\mathcal{D}[2]$-multiplet [49]. The highest-weight state of this multiplet is an adjoint-valued scalar field known as the moment map, ϕ.[7] The OPE of two of these moment maps contains a contribution from the $\mathcal{D}[2]$ multiplet, with OPE coefficient $\lambda_{\mathcal{D}[2]} = \lambda_{\phi\phi\mathcal{D}[2]}$. This coefficient is related to the flavor central charge [40], via the definition in equation (4):

$$C_J = \frac{5h^\vee}{\lambda^2_{\mathcal{D}[2]}} \,, \tag{8}$$

where $h^\vee$ is the dual Coxeter number of the flavor algebra. Upper bounds on $\lambda^2_{\mathcal{D}[2]}$ – and thus lower bounds on C_J – can be determined from the superconformal bootstrap, to which we turn in Section III.

---

[4] A recent summary on the determination of anomaly polynomials of 6d SCFTs appears in [47]. We refer to that paper for the conventions used herein.

[5] There is a slight difference in normalization with respect to [48]: $C_J(\text{us}) = \mathrm{vol}(S^5)^2\, C_J(\text{them})$.

[6] The normalization differs from that of [40] by a factor of two.

[7] The highest-weight state of a $\mathcal{D}[2J_R]$-multiplet transforms in the $SU(2)_R$ representation with highest weight $(2J_R)$ and has conformal dimension $\Delta = 4J_R$. Thus, the moment map transforms in the adjoint representation of both $SU(2)_R$ and the flavor symmetry.

Another interesting feature of a 6d SCFT, and one which can be gainfully employed in a superconformal bootstrap approach, is the associated Higgs branch. This is the hyperkähler moduli space where the half-BPS states gain vacuum expectation values and as such it is a more refined property than the numerical value of C_J. It is not known how to determine the Higgs branch in general. If the 6d SCFT admits a Type IIA description however, then the methods of magnetic quivers [50] can be used. Fortunately, minimal (D_k, D_k) conformal matter possesses such a Type IIA description, and their magnetic quivers were studied in [44, 51].

One must distinguish the Higgs branch of the tensor-branch theory from that of the conformal fixed point. In either case, the structure of the Higgs branch is preserved by dimensional reduction and it can be studied using the associated 3d magnetic quivers. In the former case, the Higgs branch is the closure of the nilpotent orbit of $\mathfrak{so}_{4k}$ associated to the partition $[2^{2k-8}, 1^{16}]$ of $4k$, and the Higgs branch chiral ring is finitely-generated by the moment map operator. Typically the chiral ring is not freely generated and the presence of chiral-ring relations is determined from the Hilbert series, which, in turn, can be computed from the magnetic quiver. Due to the half-BPS states arising from the tensionless strings, the dimension of the Higgs branch jumps by 29 when one travels to the origin of the tensor branch. A new generator of the chiral ring appears at the SCFT point, and it transforms in one of the spinor representations of $\mathfrak{so}_{4k}$ with R-charge $2J_R = k - 2$.

The Hilbert series (HS) encodes which of the flavor representations are allowed to appear in chiral-ring relations involving a spin-J_R representation of $SU(2)_R$. Any flavor symmetry representation that does not appear in the Hilbert series at order t^{2J_R} implies that the theory does not contain a $\mathcal{D}[2J_R]$ superconformal multiplet transforming in that representation. Denoting the irreducible representations of $\mathfrak{so}_{4k}$ appearing in $\mathbf{adj}\otimes\mathbf{adj}$ by $\mathcal{R}_i$ (as in Figure 1), one finds the following universal contributions to the Hilbert series at the conformal point:

$$\begin{aligned}\mathrm{HS}(t) &= \sum_{J_R\geq 0} c_{J_R} t^{2J_R} \\ &= (\mathcal{R}_1) + (\mathcal{R}_5)t^2 + (\mathcal{R}_1 + \mathcal{R}_3 + \mathcal{R}_4)t^4 + \cdots ,\end{aligned} \tag{9}$$

with $\mathcal{R}_1 = \mathbf{1}$ and $\mathcal{R}_5 = \mathbf{adj}$. The ellipses indicate terms with $J_R > 2$ or other representations that do not appear in the $\mathbf{adj}\otimes\mathbf{adj}$ decomposition. For instance, the presence of the second generator might lead to extra cubic or quadratic terms in the Hilbert series, but these are not relevant for our purposes.

An important consequence of this analysis is that the unit operator and the moment map can only transform in the singlet or adjoint representations respectively, as expected, and furthermore that half-BPS states with $J_R = 2$ are forbidden to transform in the representations $\mathcal{R}_i\,, i = 2, 5, 6$. We will see in Section IV that this selection rule will provide an additional cross-check to the claim that conformal matter saturates unitarity bounds.

III. THE CONFORMAL BOOTSTRAP

The conformal bootstrap relies on the associativity of the OPE and the decomposition of four-point correlation functions in terms of (super)conformal blocks to extract constraints on the spectrum. The majority of bootstrap studies focus on correlation functions of Lorentz scalars; the structure of their OPE and the conformal blocks being well understood in those cases [52–54]. As we are interested in obtaining bounds on theories with flavor symmetry $\mathfrak{so}_{4k}$, we use that the moment map is a Lorentz scalar, as seen in Section II. For 6d SCFTs with eight supercharges, the sum rules used in the conformal bootstrap were first derived in [38] and applied to theories with $\mathfrak{f} = \mathfrak{e}_8$ flavor symmetry, which we now review with minor modifications for the case where $\mathfrak{f} = \mathfrak{so}_{4k}$.

In order to avoid cluttering due to the proliferation of R-symmetry indices, it is customary to introduce an auxiliary variable $Y^A\,, A = 1, 2$, and define degree-two homogeneous functions, $\phi^a(x, Y) = \phi^a(x)_{AB} Y^A Y^B$. The correlation functions of four of these operators are then constrained by symmetry to take the form [55]:

$$\begin{aligned}\left\langle \phi^a(x_1, Y_1)\phi^b(x_2, Y_2)\phi^c(x_3, Y_3)\phi^d(x_4, Y_4)\right\rangle = \\ \frac{(Y_1\cdot Y_2)^2(Y_3\cdot Y_4)^2}{x_{12}^8 x_{34}^8} G^{abcd}(u, v; w)\,.\end{aligned} \tag{10}$$

The three variables u, v, w are called the cross-ratios, and are invariant under conformal and $SU(2)_R$ transformations:

$$\begin{aligned} u = \frac{x_{12}^2 x_{34}^2}{x_{13}^2 x_{24}^2}\,, \quad v = \frac{x_{14}^2 x_{23}^2}{x_{13}^2 x_{24}^2}\,, \\ w = \frac{(Y_1\cdot Y_2)(Y_3\cdot Y_4)}{(Y_1\cdot Y_4)(Y_2\cdot Y_3)}\,, \\ x_{pq}^2 = |x_p - x_q|^2\,, \quad Y_p\cdot Y_q = \epsilon_{AB} Y_p^A Y_q^B\,. \end{aligned} \tag{11}$$

The four-point function must also be a four-index invariant tensor of the flavor symmetry. The conformal- and $SU(2)_R$-invariant part of the correlation function, $G^{abcd}(u, v; w)$, can therefore further be decomposed into a sum over the projectors onto irreducible representations $\mathcal{R}_i$ appearing in $\mathbf{adj}\otimes\mathbf{adj}$ [56]:

$$G^{abcd}(u, v; w) = \sum_{\mathcal{R}_i\in\mathbf{adj}\otimes\mathbf{adj}} P_i^{abcd}\, G_i(u, v; w)\,. \tag{12}$$

The tensors P_i^{abcd} are the projectors onto $\mathcal{R}_i$ and satisfy the usual properties [57]:

$$P_i^{abcd} P_j^{dcef} = \delta_{ij} P_i^{abef}\,, \qquad P_i^{abba} = \dim(\mathcal{R}_i)\,. \tag{13}$$

Having broken down the four-point function into invariants for each of the flavor symmetry channels $G_i(u, v; w)$, we further decompose it into contributions from each of the superconformal multiplets, χ, appearing in the OPE

of two moment maps and transforming in a given irreducible representation $\mathcal{R}_i$ of the flavor symmetry:

$$G_i(u,v;w) = \sum_{\substack{\chi\in\phi\times\phi\\ \chi \text{ in } \mathcal{R}_i}} \lambda^2_{\chi,\mathcal{R}_i}\mathcal{G}_\chi(u,v;w)\,. \tag{14}$$

For ease of notation, we write the OPE coefficients of $\chi \in \phi\times\phi$ as $\lambda_{\phi\phi\chi} = \lambda_\chi$. The superconformal blocks, $\mathcal{G}_\chi(u,v;w)$, can themselves be expanded as a linear combination over the non-supersymmetric conformal blocks associated to the bosonic primaries in the superconformal multiplet, and they satisfy both a Casimir differential equation [58] and a Ward identity [55, 59]. This allows one to write each coefficient as a rational function depending solely on the quantum numbers of the superconformal primary. For theories with eight supercharges and $2 < d \leq 6$, this analysis was performed in detail for the moment map in [40, 58] and generalized to arbitrary $\mathcal{D}$-type half-BPS multiplets in [60], to which we refer for the exact expressions.

In addition to the form of the superconformal blocks, it was also found that not all types of superconformal multiplets are allowed to appear in the OPE. Let us denote a superconformal multiplet by $\chi[2J_R]_{\Delta,\ell,\mathcal{R}}$. For 6d SCFTs with $\mathcal{N} = (1,0)$ supersymmetry, the multiplets can be long, $\chi = \mathcal{L}$, or short, $\chi = \mathcal{A},\mathcal{B},\mathcal{C},\mathcal{D}$ [49, 61]. In the present case, the superconformal primary always transforms in the ℓ-traceless symmetric representation of the Lorentz group and has integer R-charge J_R.[8] It has conformal dimension Δ, while $\mathcal{R}$ indicates the representation under the flavor symmetry. For short multiplets, the superconformal primary is annihilated by a particular subset of the supercharges, fixing some of its quantum numbers. In those cases, we drop the associated subscript. For instance, $\mathcal{D}[2J_R]$-type superconformal primaries are half-BPS and must be scalars ($\ell = 0$) of conformal dimension $\Delta = 4J_R$.

It turns out that $\mathcal{A}$- and $\mathcal{C}$-type multiplets cannot appear in the decomposition in equation (14), while long multiplets must be R-symmetry singlets. Generically, only the following multiplets are allowed:[9]

$$\begin{array}{ccc} \mathcal{L}[0]_{\Delta,\ell,\mathcal{R}}\,, & \mathcal{B}[0]_{0,\mathcal{R}}\,, & \mathcal{B}[2]_{\ell,\mathcal{R}}\,, \\ \mathcal{D}[0]_{\mathbf{1}}\,, & \mathcal{D}[2]_{\mathbf{adj}}\,, & \mathcal{D}[4]_{\mathcal{R}}\,. \end{array} \tag{15}$$

The unit operator, $\mathcal{D}[0]$, and the moment-map superconformal multiplet, $\mathcal{D}[2]$, must transform in the singlet and adjoint representations of the flavor symmetry, respectively, as we also observed from the Hilbert series in equation (9). We denote a generic superconformal multiplet transforming in a representation $\mathcal{R}$ of the flavor symmetry as $\chi_\mathcal{R}$ when the other quantum numbers are not relevant.

Having a block decomposition of the four-point function, the important observation that led to the conformal bootstrap is that performing an OPE in either of the s, t, or u channels does not change its structure. Using the properties of superconformal blocks under exchange of kinematic variables,

$$(1\leftrightarrow 2):\; G_i(u,v;w) = (-1)^{|\mathcal{R}_i|}\,G_i(\frac{u}{v},\frac{1}{v};\frac{-w}{w+1})\,, \tag{16}$$

$$(1\leftrightarrow 3):\; G_i(u,v;w) = \left(\frac{u^2}{v^2 w}\right)^2 G_i(v,u;w^{-1})\,, \tag{17}$$

one then obtains two sets of constraints from the crossing symmetry of the four-point function [40].

In the specific case of the moment map, invariance under exchange of $(x_1,Y_1,a)\leftrightarrow(x_2,Y_2,b)$ leads to an additional selection rule: a superconformal multiplet can only appear in the conformal block decomposition if its quantum numbers satisfy:

$$\ell + J_R + |\mathcal{R}_i| \in 2\mathbb{Z}\,, \tag{18}$$

where $|\mathcal{R}_i|$ is defined as the parity of the embedding of $\mathcal{R}_i$ in $\mathbf{adj}\otimes\mathbf{adj}$, specifically 0 or 1 if the representation is embedded symmetrically or anti-symmetrically, respectively. In Figure 1, we give the decomposition into irreducible representations for $\mathfrak{so}_{4k}$ and the relevant group-theoretic quantities.

On the other hand, invariance under the exchange $(x_1,Y_1,a)\leftrightarrow(x_3,Y_3,c)$, in combination with equations (12) and (17), leads to the following constraint:

$$F_i{}^j G_j(u,v;w) = \frac{u^4}{v^4 w^2} G_i(v,u;w^{-1})\,. \tag{19}$$

The crossing matrix, $F_i{}^j$, captures how the flavor representations are reshuffled when going from the s channel to the t channel. The indices i,j run over the irreducible representations $\mathcal{R}_i$ inside of $\mathbf{adj}\otimes\mathbf{adj}$. The matrix is defined via the following combination of the projectors [56]:

$$F_i{}^j = \frac{1}{\dim(\mathcal{R}_i)} P_i^{dabc} P_j^{abcd}\,, \qquad F_i{}^k F_k{}^j = \delta_i^j\,. \tag{20}$$

It is therefore a purely group-theoretic quantity, and for $\mathfrak{f} = \mathfrak{so}_n$, using "birdtrack" techniques [57], a lengthy but straightforward computation leads to the results collated in Figure 1.

While the crossing matrix deals with the flavor symmetry, we still need to decompose the constraint in equation (19) into each R-symmetry channel. Invariance under the R-symmetry forces the function $G_i(u,v;w)$ to be a degree-two polynomial in w^{-1} [55]:

$$G_i(u,v;w) = \sum_{k=0}^{2} G_i^{(k)}(u,v) w^{-k}\,. \tag{21}$$

---

[8] Generically, the superconformal multiplets depend on all three Dynkin indices of $\mathfrak{so}_6$, but for OPEs of scalars, we are restricted to $[0,\ell,0]$ representations.

[9] Type $\mathcal{B}[0]_{\ell>0}$ multiplets are in principle also allowed in the OPE, but they include higher-spin conserved currents. The presence of these multiplets in the spectrum implies that (at least a subsector of) the theory is free [49, 61, 62]. We exclude them as we focus on interacting SCFTs.

$$
\begin{array}{rcccccccccc}
\mathbf{adj}\otimes\mathbf{adj} = \mathcal{R}_1 & \oplus & \mathcal{R}_2 & \oplus & \mathcal{R}_3 & \oplus & \mathcal{R}_4 & \oplus & \mathcal{R}_5 & \oplus & \mathcal{R}_6 \\
\dim\mathcal{R}_i & : & 1 & + \frac{(n-1)(n+2)}{2} & + \frac{(n-3)n(n+1)(n+2)}{12} & + \frac{n(n-1)(n-2)(n-3)}{24} & + \frac{n(n-1)}{2} & + \frac{n(n+2)(n-1)(n-3)}{8} \\
|\mathcal{R}_i| & : & + & + & + & + & - & -
\end{array}
$$

$$
F_i{}^j = \begin{pmatrix}
\frac{2}{n(n-1)} & \frac{n+2}{n} & \frac{(n-3)(n+1)(n+2)}{6(n-1)} & \frac{(n-3)(n-2)}{12} & 1 & \frac{(n-3)(n+2)}{4} \\
\frac{2}{n(n-1)} & \frac{n^2-8}{2(n-2)n} & \frac{(n-4)(n-3)(n+1)}{6(n-2)(n-1)} & \frac{3-n}{6} & \frac{n-4}{2(n-2)} & -\frac{n-3}{n-2} \\
\frac{2}{n(n-1)} & \frac{n-4}{(n-2)n} & \frac{n^2-6n+11}{3(n-2)(n-1)} & \frac{1}{6} & -\frac{1}{n-2} & -\frac{n-4}{2(n-2)} \\
\frac{2}{n(n-1)} & -\frac{2(n+2)}{(n-2)n} & \frac{(n+1)(n+2)}{3(n-2)(n-1)} & \frac{1}{6} & \frac{2}{n-2} & -\frac{n+2}{2(n-2)} \\
\frac{2}{n(n-1)} & \frac{(n-4)(n+2)}{2(n-2)n} & -\frac{(n-3)(n+1)(n+2)}{6(n-2)(n-1)} & \frac{n-3}{6} & \frac{1}{2} & 0 \\
\frac{2}{n(n-1)} & -\frac{4}{(n-2)n} & -\frac{(n-4)(n+1)}{3(n-2)(n-1)} & -\frac{1}{6} & 0 & \frac{1}{2}
\end{pmatrix}
$$

FIG. 1: Decomposition of $\mathbf{adj}\otimes\mathbf{adj}$ for $\mathfrak{so}_n$ algebras and the group-theoretic data relevant for the $\mathcal{N}=(1,0)$ sum rules with flavor. The highest-weights of the representations are $\mathcal{R}_1=\mathbf{1}:[00\cdots]$, $\mathcal{R}_2:[20\cdots]$, $\mathcal{R}_3:[020\cdots]$, $\mathcal{R}_4:[00010\cdots]$, $\mathcal{R}_5=\mathbf{adj}:[010\cdots]$, and $\mathcal{R}_6:[1010\cdots]$.

Using the relation in equation (17) one find constraints for each power of w, but, as pointed out in [40], they are not independent. Using the superconformal Ward identity, it is then possible to find a single independent constraint for each flavor-representation channel. These constraints are referred to as the *sum rules*, and are given by:

$$
\sum_{\substack{\chi\in\phi\times\phi \\ \chi \text{ in } \mathcal{R}_j}} \lambda^2_{\chi,\mathcal{R}_j}\left(F_i{}^j\mathcal{K}_\chi(u,v)-\delta_i^j\mathcal{K}_\chi(v,u)\right)=0\,, \tag{22}
$$

where the sum is over each multiplet that transforms in the representation $\mathcal{R}_j\in\mathbf{adj}\otimes\mathbf{adj}$, subject to the selection rule in equation (18). Furthermore, we have defined the function

$$
\mathcal{K}_\chi(u,v)=v^4\mathcal{G}^{(2)}_\chi(u,v)-u^4\mathcal{G}^{(0)}_\chi(v,u)\,, \tag{23}
$$

and used a polynomial expansion of the superconformal blocks similar to that of equation (21),[10]

$$
\mathcal{G}_\chi(u,v;w)=\sum_{k=0}^{2}\mathcal{G}^{(k)}_\chi(u,v)w^{-k}\,. \tag{24}
$$

We refer to [40, 58, 60] for additional details on the derivations of the sum rules and the form of the conformal blocks.

[10] In the notation using the auxiliary R-symmetry variable, a possible decomposition for the superconformal blocks of a multiplet, χ, is in terms of Legendre polynomials, P_n:

$$
\mathcal{G}_\chi(u,v;w)=\sum_{(\Delta,\ell,J)\in\chi}c_{\Delta,\ell,J}P_{2J}(1+2/w)g_{\Delta,\ell}\,,
$$

where $g_{\Delta,\ell}$ are the bosonic conformal blocks, and the sum is taken over the bosonic (conformal but not necessarily superconformal) primaries in χ. While convenient to derive the explicit expression of $\mathcal{G}_\chi$, we stress that this basis is different from the one used in equation (21).

IV. BOOTSTRAPPING CONFORMAL MATTER

To extract constraints on the spectrum of the SCFT from the sum rules in equation (22), we use the now-standard linear-functional method introduced in [17], which we briefly summarize here. The interested reader will find additional details in the reviews [63–67].

Consider the space of functions of the conformal cross-ratios, $f(u,v)$. We may then define a functional, α_i, for each of the flavor channels. The space of such linear functionals can be parameterized by linear combinations of derivatives of the function evaluated at, for instance, the crossing-symmetric point, $u=v$:

$$
\alpha^i[f]=\sum_{m,n}\alpha^i_{m,n}\,\partial_u^m\partial_v^n f(u,v)|_{u=v}\,. \tag{25}
$$

Applying this functional to the sum rules and summing over all flavor channels, we obtain the single constraint

$$
\begin{aligned}
&\sum_{\chi_{\mathcal{R}_i}\in\phi\times\phi}\lambda^2_{\chi,\mathcal{R}_i}\alpha[\chi_{\mathcal{R}_i}]=0\,,\\
&\alpha[\chi_{\mathcal{R}_j}]=F_i{}^j\alpha^i[\mathcal{K}_\chi(u,v)]-\delta^j_i\alpha^i[\mathcal{K}_\chi(v,u)]\,,
\end{aligned} \tag{26}
$$

where we abuse the notation and use $\alpha[\chi_{\mathcal{R}_i}]$ to denote the linear combination of the functionals α^i applied to the function in equation (23) for a multiplet χ transforming in the representation $\mathcal{R}_i$.

By unitarity, the OPE coefficients satisfy $\lambda^2_{\chi,\mathcal{R}_i}\geq 0$, and the numerical conformal bootstrap involves searching for a functional such that:

$$
\begin{aligned}
&\alpha[\mathcal{D}[2]_{\mathbf{adj}}]=1\,;\\
&\alpha[\chi_{\mathcal{R}_i}]\geq 0\,,\qquad \forall\ \chi_{\mathcal{R}_i}\neq\mathcal{D}[0]_{\mathbf{1}}\,,\mathcal{D}[2]_{\mathbf{adj}}\,;\\
&\alpha[\mathcal{D}[0]_{\mathbf{1}}]\ \text{maximized}\,.
\end{aligned} \tag{27}
$$

Plugging back into in equation (26) and using a convention in which the OPE coefficients of the identity and moment map are normalized such that $\lambda^2_{\mathcal{D}[0],\mathbf{1}}=\dim\mathfrak{f}$ and

$\lambda^2_{\mathcal{D}[2],\mathbf{adj}} = \lambda^2_{\mathcal{D}[2]}$, we obtain an upper bound on $\lambda^2_{\mathcal{D}[2]}$ and by extension a lower bound on the flavor central charge:

$$\begin{aligned} \lambda^2_{\mathcal{D}[2]} &\leq -\alpha[\mathcal{D}[0]_{\mathbf{1}}] \dim \mathfrak{f}\,, \\ C_J &\geq \frac{5h^\vee}{-\alpha[\mathcal{D}[0]_{\mathbf{1}}] \dim \mathfrak{f}}\,, \end{aligned} \tag{28}$$

with $h^\vee = (n-2)\,, \dim \mathfrak{f} = \frac{1}{2}n(n-1)$ for $\mathfrak{f} = \mathfrak{so}_n$. Similar bounds can be obtained for any OPE coefficient by demanding the functional be normalized with respect to the relevant multiplet.

The system defined by equation (27) is called a semi-definite program, and solving it is a well-defined optimization problem. In practice, we restrict ourselves to a finite number of derivatives, up to a cutoff $2m + n \leq \Lambda$, which captures only a portion of the space of functionals. As a functional satisfying equation (27) for a given Λ is included in the space of functionals with $\Lambda + 1$, we can only find improved results as the cutoff is increased, and sending $\Lambda \to \infty$ will correspond to strongest bound.

There are nowadays standard tools to solve semi-definite programs, in particular a numerical solver, `SDPB`, was specifically created for applications to the numerical bootstrap [68, 69]. In Appendix A, we explain how we implemented and solved the semi-definite program numerically, leading to the results found in the next sections.[11]

We stress that we obtain rigorous bounds: the conformal bootstrap only relies on numerical algorithms to find the optimal coefficients $\alpha^i_{m,n}$ of the functionals defined in equation (25) satisfying equation (27). While some standard approximations are necessary, such as truncating the spin of the operators appearing in the OPE, we verified that, up to the number of significant digits presented in the next sections, our results are stable against the increase of these parameters.

A. Bounds on Central Charges

Having reviewed the sum rules for the moment map and the associated semi-definite program defined in equation (27), we have now gathered all the necessary tools to find bounds on the flavor central charge of 6d $\mathcal{N} = (1,0)$ SCFTs with $\mathfrak{f} = \mathfrak{so}_{4k}$.

From the geometric point of view, the theory with the smallest $\mathfrak{so}_{4k}$ flavor symmetry has $k = 5$ and corresponds to minimal (D_5, D_5) conformal matter. Solving the semi-definite program in equation (27), we obtain the results shown in Figure 2.

[11] The reader interested in raw data should feel free contact us.

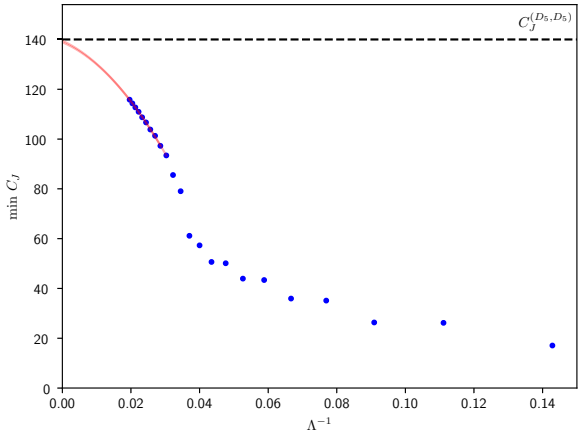

FIG. 2: Bootstrap lower bounds on C_J for theories with flavor symmetry $\mathfrak{so}_{20}$. The red lines correspond to quadratic interpolations for points with either $\Lambda \geq 33$ or $\Lambda \geq 35$. The derivative cutoffs are $\Lambda = 7, 9, \ldots, 49, 51$.

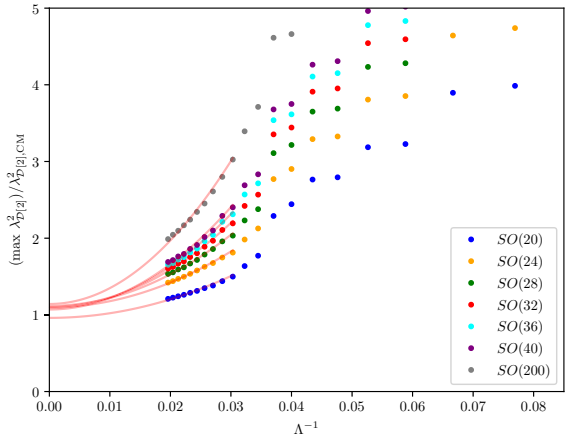

FIG. 3: Ratios between the bootstrap lower bounds on $\lambda^2_{\mathcal{D}[2]}$ with $\mathfrak{so}_{4k}$ flavor and the associated value for (D_k, D_k) conformal matter. The red lines correspond to quadratic interpolations for points with $\Lambda \geq 33$.

k	$\min C_J$	$C_J^{(D_k,D_k)}$
5	115	140
6	144	205
7	175	270
8	208	335
9	241	400
10	275	465
50	1540	3065

TABLE I: Bounds on C_J for various $\mathfrak{so}_{4k}$ flavor symmetries, and that of (D_k, D_k) conformal matter. The values for $\min C_J$ are those obtained when $\Lambda = 51$.

We can see that as the derivative cutoff Λ increases, the lower bound on C_J improves; in particular, with $\Lambda = 51$ we obtain the strict bound $C_J > 115$, ruling out any putative spectrum with a lower value of the flavor central charge.

Using quadratic fits on the last few points, we can further see that there is strong evidence that as $\Lambda \to \infty$, we will obtain the bound $\min C_J \geq C_J^{(D_5,D_5)} = 140$, indicating that minimal (D_5, D_5) conformal matter is the theory saturating the unitarity bounds.

We find that analogous results also hold for higher values of k. To aid comparison, Figure 3 shows the ratio between the bound on $\lambda^2_{\mathcal{D}[2]}$ and its value for minimal (D_k, D_k) conformal matter. As more derivatives are taken into account, this ratio approaches one, again appearing to rule out any SCFTs with a smaller flavor central charge than conformal matter. A quadratic fit further predicts that as $\Lambda \to \infty$, we approach $\min C_J = C_J^{(D_k,D_k)}$ within ten percent. The interpolation improves as larger values of Λ are taken into account, and we conjecture that minimal (D_k, D_k) conformal matter saturates the unitarity bounds for $\mathfrak{so}_{4k}$ flavor symmetry.

We emphasize again that while conformal matter has the lowest value of the flavor central charge from the geometric point of view, it is *a priori* not obvious that, purely from superconformal-field-theoretic arguments, there cannot exist another theory with $\mathfrak{f} = \mathfrak{so}_{4k}$, lying outwith the F-theory construction, satisfying $C_J < C_J^{(D_k,D_k)}$. Our results exclude a large part of those potential spectra. For instance, with $k = 50$, we rule out the existence of any theory with $C_J \leq \frac{1}{2} C_J^{(D_{50},D_{50})}$, a bound that is even more stringent for lower values of k. We have collated these bounds for $\Lambda = 51$ in Table I.

B. Low-lying Spectrum of Scalar Long Multiplets

In addition to bounding the OPE coefficient $\lambda^2_{\mathcal{D}[2]}$, the conformal bootstrap can also be used to extract the conformal dimension of long multiplets appearing in the superconformal block decomposition. This is referred to as the extremal-functional method [70], and relies on the fact that when the bound given in equation (28) is saturated, the sum rules require the associated, extremized, functional, α_E, to satisfy

$$\alpha_E[\chi] = 0\,, \qquad \forall\, \chi \neq \mathcal{D}[0]_{\mathbf{1}}\,,\, \mathcal{D}[2]_{\mathbf{adj}}\,. \tag{29}$$

Solving the constraint $\alpha_E[\mathcal{L}[0]_{\Delta,\ell,\mathcal{R}}] = 0$ for a given long multiplet, we can estimate the values of conformal dimensions. As we are operating under the assumption that the limit $\Lambda \to \infty$ corresponds to the extremal functional associated to conformal matter, for which evidence was adduced in Section III, this enables us to learn more about its spectrum.

Figures 4–7 show the functional applied to long multiplets in various flavor representations of $\mathfrak{f} = \mathfrak{so}_{4k}$ with $k = 5, 10, 50$. For the representations $\mathcal{R}_1, \mathcal{R}_2, \mathcal{R}_3$, there is a gap of at least one between the dimension of lowest-lying operator and the unitarity bound, $\Delta > 6$, for long scalar multiplets.[12] While there are variations, the position of the conformal dimensions does not appear to deviate significantly as k increases.

On the other hand for $\mathcal{R}_4$, the four-antisymmetric representation, the extremal-functional method indicates that there is an operator lying close to threshold. In that case, the functionals are close together around that point, and get closer to $\Delta = 6$ as k grows.

At threshold, long multiplets decompose (among others) into type-$\mathcal{A}$ multiplets [49, 61]. As we have reviewed in Section III, these kinds of operators are forbidden to appear in the OPE, and the anomalous dimension therefore cannot vanish. If a multiplet with such a small anomalous dimension is not an artifact of non-extremality, and there is indeed a small deviation from $\Delta = 6$, it would seem to indicate the presence of a large-k regime where perturbation theory can in principle be used. This is somewhat reminiscent of large R-charge limits, which have recently been shown to exhibit an integrable subsector [14]. It would be interesting to study whether such a large-k limit can be probed from the geometry, and whether there is a connection with integrability.

C. Chiral-ring Relations

As reviewed in Section II, (D_k, D_k) conformal matter chiral-ring relations forbid some of the $\mathcal{D}$-type superconformal multiplets to appear in certain flavor representations. Even without solving the semi-definite program in equation (27), the selection rule in equation (18) imposed by crossing symmetry is already powerful enough to prevent the presence of $\mathcal{D}[4]$ multiplets in the antisymmetric representations, $\mathcal{R}_5, \mathcal{R}_6$, as required by the chiral ring relations, see equation (9).

For symmetric representations, we expect, when we approach the unitarity bound, to find that $\alpha[\mathcal{D}[4]_{\mathcal{R}}] \to 0$ as $\Lambda \to \infty$, if the representation is allowed. In Table II, we show the numerical values of the functional for these multiplets in each of the four symmetric representations. We can see that for $\mathcal{R}_1 = \mathbf{1}$ and $\mathcal{R}_3 : [020\cdots]$, the functional is several orders of magnitude smaller than the other two representations. For comparison, in the case of the multiplet containing the stress-energy tensor, which we know appears in the OPE, we obtain values of the same order of magnitude, $\alpha[\mathcal{B}[0,0]_{\mathbf{1}}] \sim 10^{-12}$. This leads us to conclude that the $\mathcal{D}[4]$ multiplet in the two-symmetric representation of the $\mathfrak{so}_{4k}$ flavor, $\mathcal{D}[4]_{\mathcal{R}_2}$, being of order one, is forbidden to appear.

---

[12] For $k = 5$, the vanishing of $\alpha_E[\mathcal{L}[0,0]_{\mathbf{1}}]$ close to $\Delta = 6$ appears to vanish for higher values of Λ.

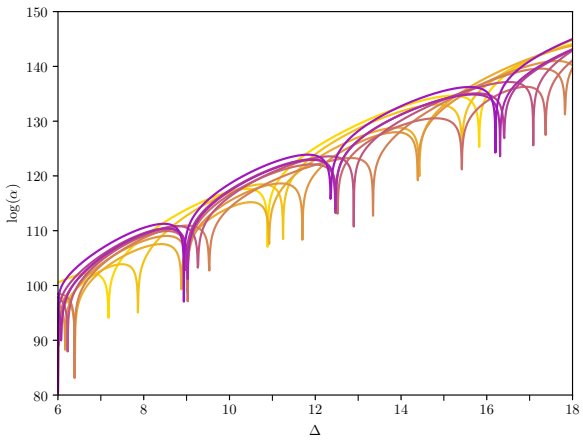

(a) $\mathfrak{so}_{20}$

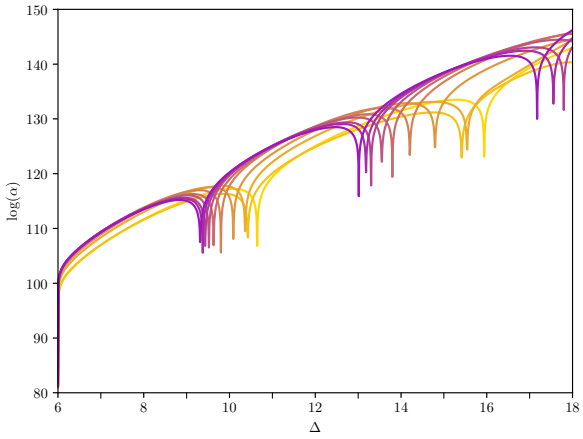

(b) $\mathfrak{so}_{40}$

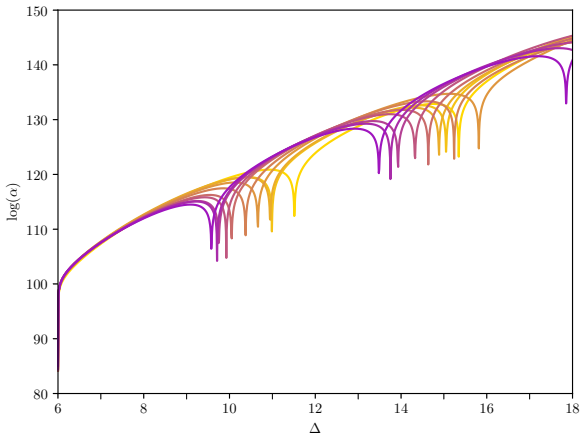

(c) $\mathfrak{so}_{200}$

FIG. 4: $\alpha[\mathcal{L}[0]_{\Delta,0,\mathbf{1}}]$ for $\Lambda = 29, 31, \cdots, 45, 47$, from gold to purple. Zeroes of the functional indicate the presence of a long multiplet at the associated Δ.

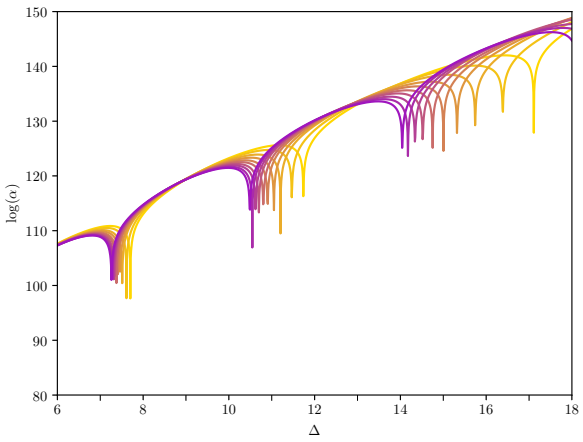

(a) $\mathfrak{so}_{20}$

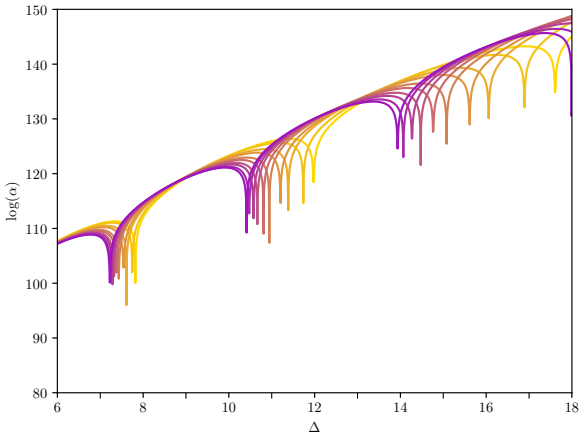

(b) $\mathfrak{so}_{40}$

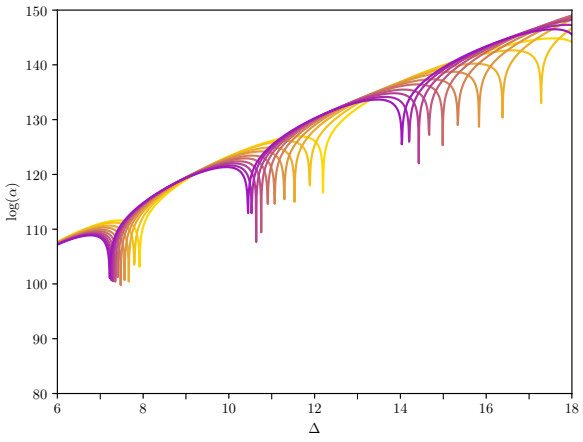

(c) $\mathfrak{so}_{200}$

FIG. 5: $\alpha[\mathcal{L}[0]_{\Delta,0,\mathcal{R}_2}]$ for $\Lambda = 29, 31, \cdots, 45, 47$, from gold to purple. Zeroes of the functional indicate the presence of a long multiplet at the associated Δ.

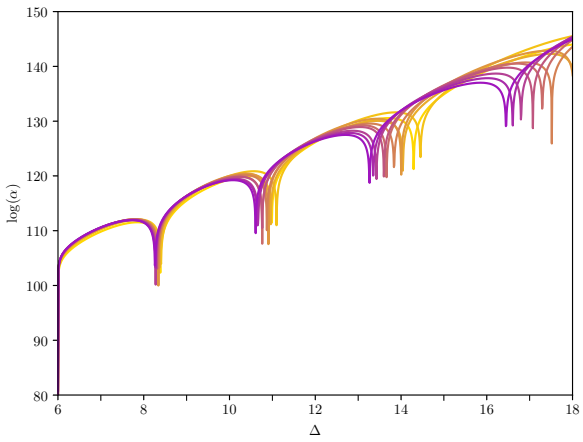

(a) $\mathfrak{so}_{20}$

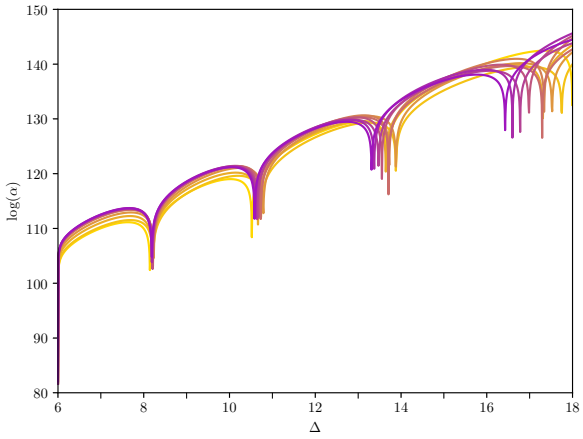

(b) $\mathfrak{so}_{40}$

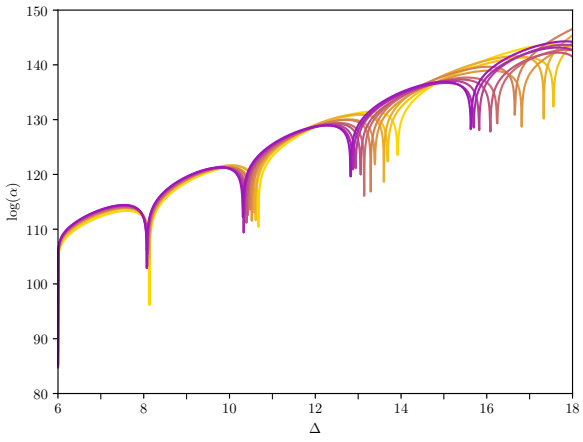

(c) $\mathfrak{so}_{200}$

FIG. 6: $\alpha[\mathcal{L}[0]_{\Delta,0,\mathcal{R}_3}]$ for $\Lambda = 29, 31, \cdots, 45, 47$, from gold to purple. Zeroes of the functional indicate the presence of a long multiplet at the associated Δ.

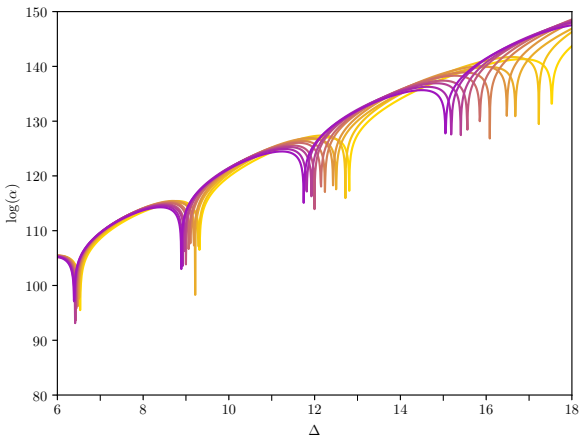

(a) $\mathfrak{so}_{20}$

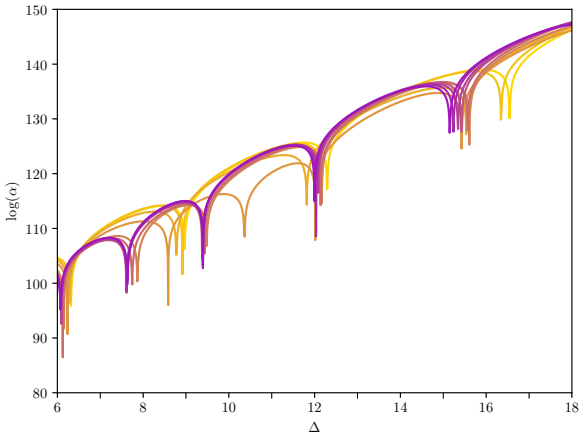

(b) $\mathfrak{so}_{40}$

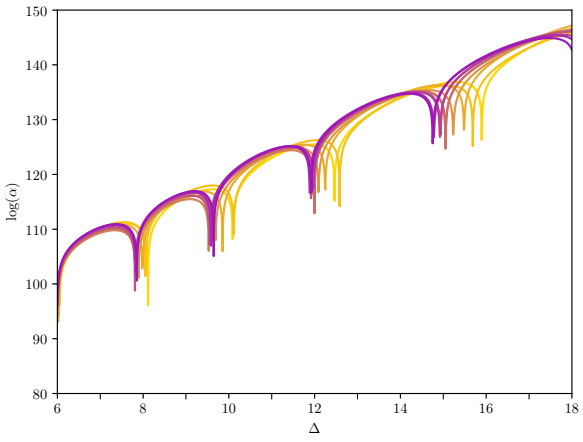

(c) $\mathfrak{so}_{200}$

FIG. 7: $\alpha[\mathcal{L}[0]_{\Delta,0,\mathcal{R}_4}]$ for $\Lambda = 29, 31, \cdots, 45, 47$, from gold to purple. Zeroes of the functional indicate the presence of a long multiplet at the associated Δ.

$\mathfrak{f}$	$\mathcal{R}_1 = \mathbf{1}$	$\mathcal{R}_2$	$\mathcal{R}_3$	$\mathcal{R}_4$
$\mathfrak{so}_{20}$	$2.7 \cdot 10^{-12}$	1.6	$2.9 \cdot 10^{-12}$	$2.0 \cdot 10^{-1}$
$\mathfrak{so}_{24}$	$2.0 \cdot 10^{-12}$	1.6	$2.5 \cdot 10^{-12}$	$4.8 \cdot 10^{-2}$
$\mathfrak{so}_{28}$	$3.6 \cdot 10^{-12}$	1.5	$4.6 \cdot 10^{-12}$	$2.0 \cdot 10^{-2}$
$\mathfrak{so}_{32}$	$6.3 \cdot 10^{-12}$	1.5	$8.3 \cdot 10^{-12}$	$1.0 \cdot 10^{-2}$
$\mathfrak{so}_{36}$	$8.5 \cdot 10^{-12}$	1.4	$1.1 \cdot 10^{-11}$	$6.0 \cdot 10^{-3}$
$\mathfrak{so}_{40}$	$8.2 \cdot 10^{-12}$	1.4	$1.1 \cdot 10^{-11}$	$3.8 \cdot 10^{-3}$
$\mathfrak{so}_{200}$	$1.6 \cdot 10^{-10}$	1.4	$2.3 \cdot 10^{-10}$	$1.7 \cdot 10^{-5}$

TABLE II: Values of $\alpha[\mathcal{D}[4]_{\mathcal{R}}]$ for $\Lambda = 49$.

As we are able to reproduce the chiral-ring condition, that $\mathcal{D}[4]$ multiplets should not appear in the representations $\mathcal{R}_2$, $\mathcal{R}_5$, or $\mathcal{R}_6$, of minimal (D_k, D_k) conformal matter, this gives even more credence to our claim that the unitarity bounds are saturated by conformal matter.

The case of $\mathcal{R}_4$, the four-antisymmetric representation, is more subtle, as the functionals seem to depend on the value of k. It appears that that for low values of k this representation is forbidden but allowed for higher values. It is very intriguing that in the case of long multiplets, the anomalous dimension was also suppressed by k for that representation. It would be interesting to further study whether $\mathcal{R}_4$ plays an important rôle for conformal matter, a question that is, to our knowledge, unexplored.

Emboldened by these results predicting the absence of half-BPS multiplets, we can endeavor to go beyond the chiral ring and use the conformal bootstrap to predict whether there are additional constraints related to $\mathcal{B}[2, \ell]$ operators, which must *a priori* only follow the selection rule in equation (18) and can therefore appear in various Lorentz and flavor representations. Figure 8 shows the value of the functional for $\mathcal{B}[2, \ell]$ as a function of the Lorentz representation, ℓ, for $\mathfrak{f} = \mathfrak{so}_{200}$.

The value of the functional grows rapidly with ℓ and it becomes difficult to comment on the presence or absence of the multiplets past the first few values. However, the value of the functional for $\mathcal{B}[2, 0]$ in the adjoint representation is significantly larger than that of $\mathcal{R}_6$. Similarly, $\mathcal{R}_1, \mathcal{R}_2$, the singlet and two-symmetric representations, are also orders of magnitude above the other symmetric representations when $\ell = 1, 3$. It is therefore tempting to conjecture that these multiplets are excluded from the OPE of two moment maps. We have checked this behaviour in several cases, and there is no indication that this potential selection rule depends on the value of k, and thus it may be valid for any minimal (D_k, D_k) conformal matter. Assuming that conformal matter saturates the bounds, it would be interesting to study whether this conjecture on the vanishing of these particular OPE coefficients can be proven directly using either field-theoretic or geometric techniques.

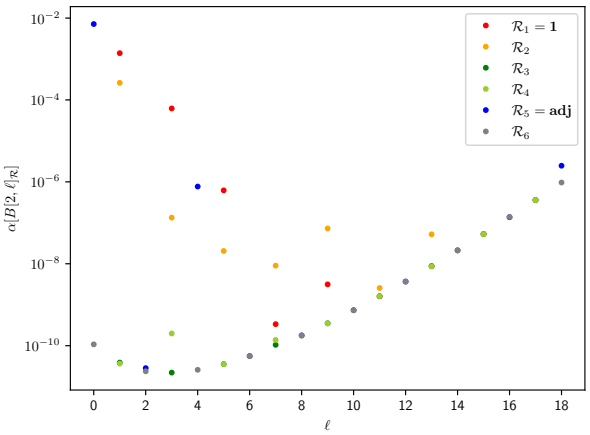

FIG. 8: Value of the functional with $\Lambda = 49$ and $\mathfrak{f} = \mathfrak{so}_{200}$ applied to $\mathcal{B}[2, \ell]_{\mathcal{R}}$ multiplets. Representations not satisfying the constraint in equation (18) do not appear in the OPE from the outset.

V. CONCLUSIONS

We have explored applications of the superconformal bootstrap to 6d SCFTs with eight supercharges, focusing on the four-point function of moment maps associated to a flavor symmetry algebra.

We extracted bounds on the flavor central charge of theories with an $\mathfrak{so}_{4k}$ symmetry, leaving little room for exotic theories with smaller central charges than minimal (D_k, D_k) conformal matter. In particular, for all the explicit values of k considered herein, we have managed to exclude the existence of a consistent theory with a flavor central charge smaller than half of that of conformal matter, a result that significantly improves with smaller values of k. For instance, when $k = 5$, the smallest possible value for (D_k, D_k) conformal matter, there is only about a ten-percent window for such theories to exist. Moreover, quadratic interpolations reasonably show that conformal matter will saturate the bounds imposed by unitarity as the whole space of functionals is explored. Using the extremal-functional method, we have checked that the value of the functional applied to half-BPS operators reproduce the expected chiral-ring relations.

We have therefore found substantial evidence that minimal (D_k, D_k) conformal matter saturates the bounds imposed by unitarity and crossing symmetry. Thus, there cannot exist any interacting 6d SCFT, with $\mathfrak{so}_{4k}$ flavor symmetry, that has a lower value of the flavor central charge; geometry determines the extremal theory!

Assuming this is indeed correct, we have extracted the low-lying spectrum of long operators, and also found new hints pointing to previously unknown selection rules for conformal matter involving $\mathcal{B}$-type multiplets. For instance, $\mathcal{B}[2, 0]$ should not appear in the OPE if it transforms in the adjoint representation, and $\mathcal{B}[2, \ell]_{\mathcal{R}_{1,2}}$ should

also be forbidden when $\ell = 1, 3$.

Our analysis exploited a peculiarity of minimal (D_k, D_k) conformal matter in that the naive flavor symmetry, $\mathfrak{so}_{2k} \oplus \mathfrak{so}_{2k}$, enhances to $\mathfrak{so}_{4k}$, so that there is only one $\mathcal{D}[2]$ superconformal multiplet. Most other types of $(\mathfrak{g}, \mathfrak{g}')$ conformal matter do not possess such an enhancement, and have two irreducible flavor currents. A natural extension of our work is therefore to consider mixed-correlator constraints involving multiple moment maps. Such bootstrap analyses have shown to be extremely powerful, and often give rise to "islands" in parameter space. Considering our results, it is natural to expect those islands to correspond to minimal $(\mathfrak{g}, \mathfrak{g})$ conformal matter and their higher-rank generalizations. Furthermore, the sum rules for mixed $\mathcal{D}[2J_R]$ correlators have been found in [60]. When $J_R > 1$ there is more than one independent sum rule, which should lead to more constraining results. While the moment map is forced to transform in the adjoint representation of the flavor symmetry, there are no such requirements for other half-BPS states. This opens the way for flavor-independent analyses, as well as bootstrap approaches to the whole chiral ring.

Our results have potential consequences beyond six dimensions. Compactifying 6d $(1, 0)$ SCFTs on a T^2 gives rise to 4d SCFTs with eight supercharges. Starting with conformal matter one can obtain a variety of 6d SCFTs by performing deformations and renormalization-group flows [71, 72]. In [47], these Higgs-branch deformations, their compactifications on T^2, and their duality with the class-$\mathcal{S}$ construction were studied; this results in a collection of 4d $\mathcal{N} = 2$ SCFTs with diverse flavor symmetry algebras for which the central charges were determined explicitly. Compactifying minimal (D_k, D_k) conformal matter on a circle, together with holonomies along the S^1, also leads to a vast collection of 5d SCFTs, for which the flavor symmetries were worked out in [73–75]. As with 6d SCFTs, not much of the conformal data is known for these theories, although it is reasonable to expect a dependence on the 6d progenitors, and again a conformal bootstrap approach may be useful.

Finally, we have found that the anomalous dimension of long multiplets transforming in the four-antisymmetric representation $\mathcal{R}_4$ of $\mathfrak{so}_{4k}$ appears to be suppressed by k. It has recently been shown that in a large R-charge limit, the anomalous dimensions in a particular subsector are controlled by an integrable spin chain [14, 76]. It would be interesting to see if we can learn more about these long multiplets using perturbation theory, and whether there is an equivalent sector in the large-k limit where integrability techniques can be used.

ACKNOWLEDGMENTS

We thank Michael Fuchs for collaboration at an early stage of this work. We are also grateful to Connor Behan, Chi-Ming Chang, Marc Gillioz, Ying-Hsuan Lin, David Simmons-Duffin, and Alessandro Vichi for helpful discussions and insights on the numerical implementation of the semi-definite programs. We thank Jonathan Heckman, Monica Jinwoo Kang, and Jaewon Song for comments and discussion on an early version of the manuscript. The numerical computations in this work were performed on the Hydra cluster of the Instituto de Física Teórica at the Universidad Autónoma de Madrid, and the General Purpose Cluster (GPC) supported by the School of Arts and Sciences at the University of Pennsylvania. F. B. is supported by the Swiss National Science Foundation (SNSF) grant number P400P2_194341. The work of C. L. was supported by a University Research Foundation grant at the University of Pennsylvania and DOE (HEP) Award DE-SC0021484, and by DESY (Hamburg, Germany), a member of the Helmholtz Association HGF.

Appendix A: Numerical Implementation

As we have reviewed in Section III, the basic elements of the numerical conformal bootstrap are the bosonic conformal blocks, $g_{\Delta,\ell}(u, v)$, and their derivatives at the point $u = v$. To solve the semi-definite program in equation (27), we made use of the rational approximation of the blocks, $\partial_u^m \partial_v^n g_{\Delta,\ell}(u, v)|_{u=v} \sim \chi_\ell(\Delta) P_\ell^{m,n}(\Delta)$ [77, 78]. The prefactor $\chi(\Delta)$ is positive for any value of the conformal dimension above the unitarity bound, and $P(\Delta)$ is a polynomial in the conformal dimension. The derivatives satisfy recursion relations found in [77, 79, 80] which can be efficiently utilized to find the rational approximation at any derivative order. We note that these relations are simpler in terms of the standard pair of variables (a, b), see e.g. [66]. In practice, we have therefore rewritten the sum rules in equation (22) in terms of these variables rather than the usual cross-ratios, (u, v).

Moreover, when evaluated at the crossing-symmetric point some of the derivatives of $\mathcal{K}$ are related by a sign: $\partial_u^m \partial_v^n \mathcal{K}(u, v)|_{u=v} = (-1)^{m+n+1} \partial_u^m \partial_v^n \mathcal{K}(v, u)|_{u=v}$. This introduces flat directions which can lead to numerical instabilities. These can be made manifest by rewriting the sum rule in terms of the eigenspaces of the flavor matrix, i.e. the projectors $P^\pm = \frac{1}{2}(\mathbf{1} \mp F)$, see for instance [25, 56].

The rational approximation of the bosonic blocks and their recursion relations have been implemented in `scalar_blocks` [81], with the value of the cut-off being related to the parameter $n_{\max}$ by $\Lambda = 2n_{\max} - 1$. We found the following parameters adequate for $n_{\max} \leq 24$ in all the cases discussed in this work:

```
poles=20
order=80
prec=1024
```

For $n_{\max} = 25, 26$, an increased precision of `1280` and `keptPoleOrder=40` are needed to ensure stable results. One also needs to introduce a cutoff for the spins, $\ell < \ell_{\max}$, of the multiplets appearing in the sum rules. We

have tested various cases and found that at $\ell_{\max} = 66$, the results are stable up to a sufficient number of significant digits.

The bounds are then obtained from the semi-definite program in equation (27) using the solver `sdpb` [68, 69] (version `2.3.1`) with parameters:

```
--dualityGapThreshold=1e-10
--maxComplementarity=1e+80
--initialMatrixScalePrimal=1e+20
--initialMatrixScaleDual=1e+20
```

The precision was the same as that used to create the bosonic blocks. The other parameters were set to their default value. We refer to the original works and the documentation of both `scalar_blocks` and `sdbp` for additional details on the numerics and the meaning of the parameters.

To test our implementation we have reproduced various results in the literature, in particular those of six-dimensional $\mathcal{N} = (1, 0)$ theories, where we have replicated the bounds found in [38] for the E-string and a free hypermultiplet.

[1] W. Nahm, Nucl. Phys. B **135**, 149 (1978).
[2] C. Cordova, T. T. Dumitrescu, and K. Intriligator, JHEP **11**, 135 (2016), arXiv:1602.01217 [hep-th].
[3] E. Witten, in *STRINGS 95: Future Perspectives in String Theory* (1995) arXiv:hep-th/9507121.
[4] N. Seiberg, Phys. Lett. B **390**, 169 (1997), arXiv:hep-th/9609161.
[5] J. J. Heckman, D. R. Morrison, and C. Vafa, JHEP **05**, 028 (2014), [Erratum: JHEP06,017(2015)], arXiv:1312.5746 [hep-th].
[6] J. J. Heckman, D. R. Morrison, T. Rudelius, and C. Vafa, Fortsch. Phys. **63**, 468 (2015), arXiv:1502.05405 [hep-th].
[7] M. Del Zotto, J. J. Heckman, A. Tomasiello, and C. Vafa, JHEP **02**, 054 (2015), arXiv:1407.6359 [hep-th].
[8] Y. Tachikawa, JHEP **06**, 128 (2016), arXiv:1508.06679 [hep-th].
[9] L. Bhardwaj, D. R. Morrison, Y. Tachikawa, and A. Tomasiello, JHEP **08**, 138 (2018), arXiv:1805.09070 [hep-th].
[10] K. Ohmori, H. Shimizu, Y. Tachikawa, and K. Yonekura, JHEP **12**, 131 (2015), arXiv:1508.00915 [hep-th].
[11] D. R. Morrison and T. Rudelius, Fortsch. Phys. **64**, 645 (2016), arXiv:1605.08045 [hep-th].
[12] H. Shimizu, Y. Tachikawa, and G. Zafrir, JHEP **12**, 127 (2017), arXiv:1703.01013 [hep-th].
[13] J. J. Heckman, Phys. Lett. B **747**, 73 (2015), [Erratum: Phys.Lett.B 808, 135675 (2020)], arXiv:1408.0006 [hep-th].
[14] F. Baume, J. J. Heckman, and C. Lawrie, Nucl. Phys. B **967**, 115401 (2021), arXiv:2007.07262 [hep-th].
[15] S. Ferrara, A. F. Grillo, and R. Gatto, Annals Phys. **76**, 161 (1973).
[16] A. M. Polyakov, Zh. Eksp. Teor. Fiz. **66**, 23 (1974).
[17] R. Rattazzi, V. S. Rychkov, E. Tonni, and A. Vichi, JHEP **12**, 031 (2008), arXiv:0807.0004 [hep-th].
[18] S. M. Chester, J. Lee, S. S. Pufu, and R. Yacoby, JHEP **09**, 143 (2014), arXiv:1406.4814 [hep-th].
[19] P. Liendo, C. Meneghelli, and V. Mitev, Commun. Math. Phys. **350**, 387 (2017), arXiv:1512.06072 [hep-th].
[20] N. B. Agmon, S. M. Chester, and S. S. Pufu, JHEP **06**, 159 (2018), arXiv:1711.07343 [hep-th].
[21] N. B. Agmon, S. M. Chester, and S. S. Pufu, JHEP **02**, 010 (2020), arXiv:1907.13222 [hep-th].
[22] C.-M. Chang, M. Fluder, Y.-H. Lin, S.-H. Shao, and Y. Wang, SciPost Phys. **10**, 097 (2021), arXiv:1910.03600 [hep-th].
[23] D. J. Binder, S. M. Chester, M. Jerdee, and S. S. Pufu, JHEP **05**, 083 (2021), arXiv:2011.05728 [hep-th].
[24] C. Beem, L. Rastelli, and B. C. van Rees, Phys. Rev. Lett. **111**, 071601 (2013), arXiv:1304.1803 [hep-th].
[25] C. Beem, M. Lemos, P. Liendo, L. Rastelli, and B. C. van Rees, JHEP **03**, 183 (2016), arXiv:1412.7541 [hep-th].
[26] L. F. Alday and A. Bissi, JHEP **02**, 101 (2015), arXiv:1404.5864 [hep-th].
[27] M. Lemos and P. Liendo, JHEP **01**, 025 (2016), arXiv:1510.03866 [hep-th].
[28] P. Liendo, I. Ramirez, and J. Seo, JHEP **02**, 019 (2016), arXiv:1509.00033 [hep-th].
[29] C. Beem, L. Rastelli, and B. C. van Rees, Phys. Rev. D **96**, 046014 (2017), arXiv:1612.02363 [hep-th].
[30] M. Lemos, P. Liendo, C. Meneghelli, and V. Mitev, JHEP **04**, 032 (2017), arXiv:1612.01536 [hep-th].
[31] P. Liendo and C. Meneghelli, JHEP **01**, 122 (2017), arXiv:1608.05126 [hep-th].
[32] I. A. Ramírez, JHEP **05**, 043 (2016), arXiv:1602.07269 [hep-th].
[33] M. Cornagliotto, M. Lemos, and P. Liendo, JHEP **03**, 033 (2018), arXiv:1711.00016 [hep-th].
[34] P. Liendo, C. Meneghelli, and V. Mitev, JHEP **10**, 077 (2018), arXiv:1806.01862 [hep-th].
[35] A. Gimenez-Grau and P. Liendo, JHEP **03**, 121 (2020), arXiv:1907.04345 [hep-th].
[36] A. Bissi, A. Manenti, and A. Vichi, JHEP **05**, 111 (2021), arXiv:2010.15126 [hep-th].
[37] A. Gimenez-Grau and P. Liendo, JHEP **01**, 175 (2021), arXiv:2006.01847 [hep-th].
[38] C.-M. Chang, M. Fluder, Y.-H. Lin, and Y. Wang, JHEP **03**, 123 (2018), arXiv:1710.08418 [hep-th].
[39] C. Beem, M. Lemos, L. Rastelli, and B. C. van Rees, Phys. Rev. D **93**, 025016 (2016), arXiv:1507.05637 [hep-th].
[40] C.-M. Chang and Y.-H. Lin, JHEP **08**, 128 (2017), arXiv:1705.05392 [hep-th].
[41] L. F. Alday, S. M. Chester, and H. Raj, JHEP **01**, 133 (2021), arXiv:2005.07175 [hep-th].
[42] J. J. Heckman and T. Rudelius, J. Phys. A **52**, 093001 (2019), arXiv:1805.06467 [hep-th].
[43] M. Bershadsky, K. A. Intriligator, S. Kachru, D. R. Morrison, V. Sadov, and C. Vafa, Nucl. Phys. B **481**, 215 (1996), arXiv:hep-th/9605200.
[44] A. Hanany and N. Mekareeya, JHEP **07**, 098 (2018), arXiv:1801.01129 [hep-th].
[45] K. Ohmori, H. Shimizu, Y. Tachikawa, and K. Yonekura, PTEP **2014**, 103B07 (2014), arXiv:1408.5572 [hep-th].

[46] K. Intriligator, JHEP **10**, 162 (2014), arXiv:1408.6745 [hep-th].

[47] F. Baume, M. J. Kang, and C. Lawrie, (2021), arXiv:2106.11990 [hep-th].

[48] C. Córdova, T. T. Dumitrescu, and K. Intriligator, JHEP **07**, 065 (2020), arXiv:1912.13475 [hep-th].

[49] C. Cordova, T. T. Dumitrescu, and K. Intriligator, JHEP **03**, 163 (2019), arXiv:1612.00809 [hep-th].

[50] A. Hanany and E. Witten, Nucl. Phys. B **492**, 152 (1997), arXiv:hep-th/9611230.

[51] G. Ferlito, A. Hanany, N. Mekareeya, and G. Zafrir, JHEP **07**, 061 (2018), arXiv:1712.06604 [hep-th].

[52] F. A. Dolan and H. Osborn, Nucl. Phys. **B599**, 459 (2001), arXiv:hep-th/0011040 [hep-th].

[53] F. A. Dolan and H. Osborn, Nucl. Phys. **B678**, 491 (2004), arXiv:hep-th/0309180 [hep-th].

[54] F. A. Dolan and H. Osborn, (2011), arXiv:1108.6194 [hep-th].

[55] F. A. Dolan, L. Gallot, and E. Sokatchev, JHEP **09**, 056 (2004), arXiv:hep-th/0405180.

[56] R. Rattazzi, S. Rychkov, and A. Vichi, J. Phys. A **44**, 035402 (2011), arXiv:1009.5985 [hep-th].

[57] P. Cvitanovic, *Group theory: Birdtracks, Lie's and exceptional groups* (2008).

[58] N. Bobev, E. Lauria, and D. Mazac, JHEP **07**, 061 (2017), arXiv:1705.08594 [hep-th].

[59] F. A. Dolan and H. Osborn, Nucl. Phys. B **629**, 3 (2002), arXiv:hep-th/0112251.

[60] F. Baume, M. Fuchs, and C. Lawrie, JHEP **11**, 164 (2019), arXiv:1908.02768 [hep-th].

[61] M. Buican, J. Hayling, and C. Papageorgakis, JHEP **11**, 091 (2016), arXiv:1606.00810 [hep-th].

[62] J. Maldacena and A. Zhiboedov, J. Phys. A **46**, 214011 (2013), arXiv:1112.1016 [hep-th].

[63] J. D. Qualls, (2015), arXiv:1511.04074 [hep-th].

[64] S. Rychkov, *EPFL Lectures on Conformal Field Theory in $\geq$ 3 Dimensions*, Briefs in Physics (Springer, 2016) arXiv:1601.05000 [hep-th].

[65] D. Simmons-Duffin, in *Proceedings, Theoretical Advanced Study Institute in Elementary Particle Physics: New Frontiers in Fields and Strings (TASI 2015): Boulder, CO, USA, June 1-26, 2015* (2017) pp. 1–74, arXiv:1602.07982 [hep-th].

[66] D. Poland, S. Rychkov, and A. Vichi, Rev. Mod. Phys. **91**, 015002 (2019), arXiv:1805.04405 [hep-th].

[67] S. M. Chester, (2019), arXiv:1907.05147 [hep-th].

[68] D. Simmons-Duffin, JHEP **06**, 174 (2015), arXiv:1502.02033 [hep-th].

[69] W. Landry and D. Simmons-Duffin, (2019), arXiv:1909.09745 [hep-th].

[70] S. El-Showk and M. F. Paulos, Phys. Rev. Lett. **111**, 241601 (2013), arXiv:1211.2810 [hep-th].

[71] J. J. Heckman, D. R. Morrison, T. Rudelius, and C. Vafa, JHEP **09**, 052 (2015), arXiv:1505.00009 [hep-th].

[72] J. J. Heckman, T. Rudelius, and A. Tomasiello, JHEP **07**, 082 (2016), arXiv:1601.04078 [hep-th].

[73] F. Apruzzi, C. Lawrie, L. Lin, S. Schäfer-Nameki, and Y.-N. Wang, Phys. Lett. B **800**, 135077 (2020), arXiv:1906.11820 [hep-th].

[74] F. Apruzzi, C. Lawrie, L. Lin, S. Schäfer-Nameki, and Y.-N. Wang, JHEP **11**, 068 (2019), arXiv:1907.05404 [hep-th].

[75] F. Apruzzi, C. Lawrie, L. Lin, S. Schäfer-Nameki, and Y.-N. Wang, JHEP **03**, 052 (2020), arXiv:1909.09128 [hep-th].

[76] J. J. Heckman, Phys. Lett. B **811**, 135891 (2020), arXiv:2007.08545 [hep-th].

[77] F. Kos, D. Poland, and D. Simmons-Duffin, JHEP **06**, 091 (2014), arXiv:1307.6856 [hep-th].

[78] J. Penedones, E. Trevisani, and M. Yamazaki, JHEP **09**, 070 (2016), arXiv:1509.00428 [hep-th].

[79] S. El-Showk, M. F. Paulos, D. Poland, S. Rychkov, D. Simmons-Duffin, and A. Vichi, Phys. Rev. **D86**, 025022 (2012), arXiv:1203.6064 [hep-th].

[80] F. Kos, D. Poland, and D. Simmons-Duffin, JHEP **11**, 109 (2014), arXiv:1406.4858 [hep-th].

[81] Bootstrap Collaboration, "`scalar_blocks`," `https://gitlab.com/bootstrapcollaboration/scalar_blocks` (2020).